Silicon quantum dots delivered phthalocyanine for fluorescence guided photodynamic therapy of tumor*

Jiao-Jiao Liu(刘娇娇)[1,†], Qi Chang(常琪)[1,†], Mei-Mei Bao(鲍美美)[1], Bing Yuan(元冰)[1,‡], Kai Yang(杨恺)[1,§], and Yu-Qiang Ma(马余强)[1,2]

[1] *Center for Soft Condensed Matter Physics and Interdisciplinary Research, College of Physics, Optoelectronics and Energy, Soochow University, Suzhou* 215006, *China*

[2] *National Laboratory of Solid State Microstructures and Department of Physics, Nanjing University, Nanjing* 210093, *China*

(Received 4 May 2017; revised manuscript received 18 May 2017; published online 27 July 2017)

Imaging-guided cancer therapy provides a simultaneous tumor imaging and treatment, which helps to eliminate the excessive toxicity to the healthy tissues. For this purpose, multifunctional probes capable of both imaging and curing are needed. In this work, we synthesize water-soluble silicon quantum dots (Si QDs) smaller than 5 nm. Such Si QDs are used for delivering the hydrophobic drug phthalocyanine (Pc). The as-prepared Si/Pc nanocomposite particles show efficient transmembrane delivery into cells and feasible biocompatibility. Moreover, these composite particles emit dual-channel fluorescence signals even after cellular internalization and demonstrate robust photostability in the Si channel. More interestingly, the Si/Pc composite particles show efficient photodynamic therapy effects against tumors both *in vitro* and *in vivo*.

Keywords: silicon quantum dot, drug delivery, photodynamic therapy

PACS: 81.07.–b, 62.23.–c **DOI:** 10.1088/1674-1056/26/9/098102

1. Introduction

As an advanced therapeutic formula, imaging-guided cancer therapy (IGCT) provides targeted treatment of tumors under the guiding of the labelling probes, in order to eliminate the excessive toxicity to the surrounding normal tissues and to promote the therapeutic efficiency against cancer cells.[1–3] Particularly, the fluorescence imaging-guided cancer therapy (FIGCT) has attracted great interest due to the wide and growing applications of fluorescence in fundamental life sciences, biomedicine and bioengineering fields.[4–6] Multifunctional probes are widely needed for both imaging and therapeutic capabilities.

A variety of strategies have been developed for multifunctional probes, such as the FITC-labeled SiO_2 nanospheres, fluorescent protein-doped gold nanoparticle capsules and fluorescent quantum dot-loaded phospholipid micelles.[7–9] However, these materials are facing challenges including the complicated procedures for carrier preparation and drug encapsulation, the large size (mostly 25–100 nm), limited cell uptake efficiency, and/or poor photostability. The semiconductor quantum dots, such as CdSe and CdTe nanoparticles, demonstrate robust fluorescence and improved photostability compared with most commercial fluorescence probes.[10–15] Nevertheless, they show inevitable cytotoxicity. Other types of particles, such as Au and Ag nanoparticles, were also developed for photothermal therapy of tumors or antimicrobial purposes.[16,17] On the other hand, compared with these heavy metal-based particles, the silicon nanostructures, including nanodots, nanowires and nanospheres, have shown feasible biocompatibility.[1,18–22] Moreover, the surface of the Si nanostructures can be easily functionalized for special purpose such as targeted tumor therapy.[18,23–25] Thus, they have been developed for biosensing, bioimaging, and tumor therapy applications. Water-dispersible Si quantum dots (Si QDs) with relatively high quantum field ($\sim 25\%$) have recently been synthesized by the reduction of (3-Aminopropyl)trimethoxysilane in aqueous solution.[12] The as-obtained Si QDs have a small size below 5 nm, which ensures them to be renally cleared *in vivo*.

Here, we would like to testify the applications of such Si QDs for FIGCT purpose. Phthalocyanine (Pc) is selected as a representative drug which has shown photodynamic therapy (PDT) effect of tumors.[26–29] As most of the anti-tumor drugs, Pc is water-insoluble and needs to be delivered into tumor cells with water-dispersible carriers. Under the irradiation of light at a certain wavelength, Pc is able to emit reactive oxygen species (ROS) to kill the tumors. Furthermore, the fluorescence emission of Pc in the biological window range with a near-infrared (NIR) wavelength promises its applications in bioimaging.

*Project supported by the National Natural Science Foundation of China (Grant Nos. 21374074, 21422404, and U1532108) and the Undergraduate Training Program for Innovation and Entrepreneurship of Soochow University, China (Grant No. 2016xj010).

†These authors contribute equally.

‡Corresponding author. E-mail: yuanbing@suda.edu.cn

§Corresponding author. E-mail: yangkai@suda.edu.cn

© 2017 Chinese Physical Society and IOP Publishing Ltd

In this paper, we will show that the hydrophobic Pc can be stably loaded to the Si QDs via facile preparation such as physical adsorption or chemical binding. The as-obtained Si QD-based composite nanoparticles show robust dual-channel fluorescence signals for imaging and obvious PDT effect of tumors both *in vitro* and *in vivo*. This work promises the possibility of the Si QDs as multifunctional probes for hydrophobic drug delivery and fluorescence-guided therapy.

2. Materials and methods

2.1. Materials

The (3-Aminopropyl)trimethoxysilane (97%), Trisodium citrate dehydrate ($\geq$ 99.0%) were purchased from Sinopharm Chemical Reagent Co., Ltd. (China). Silicon phthalocyanine dichloride (defined as Pc), LysoTracker Green DND-26 and DMSO were purchased from Sigma-Aldrich. All chemicals were used without additional purification. Milli-Q water (Millipore) was used as solvent for solution preparation. For the *in vitro* and *in vivo* tests, a stock solution of Pc in DMSO was diluted with cell culture medium or physiological saline to make sure that the cells were never exposed to more than 1% DMSO. Human gastric carcinoma cells (MGC-803) were purchased from the cell bank of the Chinese Academy of Sciences in Shanghai and cultured in Dulbecco's Modified Eagle Medium (DMEM, Hyclone) with 10% FBS in a 5% CO_2 atmosphere at 37 °C and 100% humidity.

2.2. Si QD preparation and drug loading

The pure Si QDs were firstly synthesized following our previous protocol.[12] In brief, 100 mL of (3-aminopropyl)trimethoxysilane was added into 400 mL of N_2-saturated aqueous solution containing 18.6 g trisodium citrate dehydrate and stirred for 30 min. A 15 mL of the well mixed solution was transferred to a quartz vessel, heated to 160 °C by microwave irradiation in a microwave system (at 2450 MHz frequency and 0–500 W power; Preekem of Shanghai, China). The solution was incubated at 160 °C for 3 h, and then cooled down to room temperature naturally. The obtained solution was purified by dialysis (500 Da) to remove the excessive chemicals, and concentrated by a rotary evaporator. The obtained Si QD dispersion, at a concentration of around 7.2 mg·mL^{-1} based on the UV–vis absorption measurement, was taken as mother solution for the following use.

The Si QDs were loaded with Pc by two different methods, i.e., physical adsorption and chemical binding, and referred to as (Si+Pc) and (Si∗Pc) NPs, respectively. 1) For the preparation of (Si+Pc) NPs, Pc was pre-dissolved in ethanol at 10 mg·mL^{-1} with the help of sonification. A 5 mL of the Si NP mother solution was added into 1 mL of Pc solution. The mixture was kept in the dark for 3 days with gently shaking. After that, the solution was thoroughly blown with nitrogen for fully evaporating the ethanol in the mixture and the adsorption occurred between Pc and Si via hydrophobic interaction.[19] The obtained solution was filtered through a 0.45 μm filter four times to remove the excessive Pc. The final concentration was determined to be around 6.58 mg·mL^{-1} (in respect to Si) and 1.0 mg·mL^{-1} (in respect to Pc), with a Pc-loading capacity of $\sim$ 152 mg·g^{-1}.

2) On the other hand, for the preparation of (Si∗Pc) NPs, Pc was pre-dissolved in DMSO at 10 mg·mL^{-1} by sonification. A 10 mL Si QD mother solution was dropped into 4.6 mL Pc solution slowly. The mixture was sealed, heated to 90 °C, and kept for 72 h with magnetic stirring. The amino-group on the Si QD surface is supposed to be substituted for silicon-chlorine bond with Pc in this process.[30] The solution was cooled down to room temperature naturally, purified by dialysis (500 Da) to remove the excessive chemicals, and concentrated by a rotary evaporator. The final concentration was determined to be around 9.87 mg·mL^{-1} (in respect to Si) and 1.4 mg·mL^{-1} (in respect to Pc), with a Pc-loading capacity of $\sim$ 142 mg·g^{-1}.

2.3. Characterizations

The Si, (Si+Pc), and (Si∗Pc) NP dispersions were observed in ambient light and UV irradiation (λ_{ex} = 365 nm) separately. The NPs were characterized with transmission electron microscopy (TEM; CM 200, Philips), dynamic light scattering (DLS; DynaPro, Malvern), x-ray photoelectron spectroscopy (XPS; ESCALAB 250Xi, Thermo), zeta potential (Zetasizer Nano ZS90, Malvern), UV–vis absorption (UV3600, Shimadzu) and photoluminescence (PL; FluoroMax-4, Horiba JobinYvon). A confocal laser scanning fluorescence microscope (LSM 710, Zeiss), equipped with an *in situ* cell-incubation system and a 63× oil objective, was used for fluorescence imaging. Signals from the Si channel (EX 405 nm, EM BP 445/50 nm, excited by 15% power of a diode laser), Pc channel (EX 633 nm, EM 635–750 nm, excited by 30% power of a He–Ne laser), and transmission channel (illuminated with a halogen lamp), were captured simultaneously. LysoTracker Green DND-26 was irradiated and collected in the green channel (EX 488 nm, EM BP 530/50 nm, excited by 20% power of an argon laser). All images were captured under the same instrumental settings and analyzed with image analysis software.

2.4. *In vitro* experiments

For the cellular uptake test, MGC-803 cells were pre-seeded on the cover glass substrate of a home-made unit (2×10^4 cells per unit). A certain amount of (Si+Pc), (Si∗Pc) or pure Si NP dispersion was pre-diluted with cell culture medium to the same volume and added into the unit. The system (with a final volume of 500 μL) was further incubated for a certain time duration as described in the main text. Prior to

the observation, the cells were washed with phosphate buffer saline (PBS) 3 times to remove the free NPs and re-cultured with fresh medium. To determine the intracellular localization of NPs, the cells, after NP co-incubation for 24 h, were further treated with the LysoTracker Green DND-26 (at 100 nM for 30 min), and washed prior to the confocal observation.

For the cytotoxicity test of the NPs, MGC-803 cells were pre-seeded in a 96-well plate (3000 cells per well), then co-incubated with the (Si+Pc), (Si∗Pc), pure Si NPs or free Pc at a certain concentration (from 0 to 260 μg·mL^{-1} in respect to Si or from 0 to 40 μg·mL^{-1} for free Pc; this ratio was selected based on the loading amount of Pc within the (Si+Pc) NPs) for 24 h or 48 h. The relative number of the viable cells was then evaluated by the standard MTT assay.

Photostability evaluation of the NPs was carried out *in situ* under the confocal microscope, on the cells which have been internalized with NPs and labeled with LysoTracker. The (Si+Pc) NP system was taken for example. The cells were exposed to a 488 nm irradiation by the argon laser (at 2% power) for different time intervals. Confocal images, in all the Si, Pc, and LysoTracker channels, were captured after each irradiation interval (e.g., 0, 20 min, and 40 min) with identical instrumental settings for comparison.

For the *in vitro* PDT test, the cells, which have been co-incubated with the pure Si, (Si+Pc) or (Si∗Pc) NPs for 24 h, were exposed to an NIR irradiation at 610 nm wavelength and 25 mW·cm^{-2} power for 30 min followed by PBS washing and fresh medium replacing. After that, the morphology of the cells was observed under confocal microscope and cell viability was evaluated with the established MTT assay.

2.5. *In vivo* experiments

MGC-803 tumor bearing mice were intratumorally injected with 150 μL of (Si+Pc) NP dispersion (pre-diluted with physiological saline) on the 1st day and 7th day. Physiological saline or free Pc (pre-diluted with physiological saline) with the same volume was taken as a control. The dose of Pc content was fixed at 7.5 mg·kg^{-1} (or might be lower than this value for the free Pc system due to the obvious precipitation of Pc in PBS). Four hours after each injection, the tumor area was irradiated by the 610 nm laser at 25 mW·cm^{-2} for 30 min. The tumor sizes were measured every the other day and the tumor volume V was calculated as V =(tumor length) × (tumor width)^2)/2.[31] The relative tumor volumes were normalized based on the initial value on the 1st day.

3. Results and discussion

3.1. Characterization of Pc-loaded Si NPs

The hydrophobic drug Pc was loaded to the Si NPs through physical adsorption (named (Si+Pc) NPs) and chemical binding (named (Si∗Pc) NPs) respectively. The as-obtained composite NPs in addition to the initial Si NP dispersions, were collected and characterized as shown in Fig. 1. All the three types of NP dispersions look transparent in ambient light and keep stable without apparent precipitation at 4 °C in the dark for more than three months. The (Si+Pc) and (Si∗Pc) NP dispersions present colorless while the initial Si NP dispersion shows light brown (Fig. 1(a)). Under UV irradiation, all the three dispersions show obvious photofluorescence (inset in Fig. 1(a)). Free Pc in DMSO (due to its poor solubility in water) is also shown for reference. All the three types of NPs show homogeneous size and high crystallinity under TEM and HR-TEM (Figs. 1(b) and 1(c). From the DLS test (Fig. 1(d)), the (Si+Pc) and (Si∗Pc) NPs have a little larger

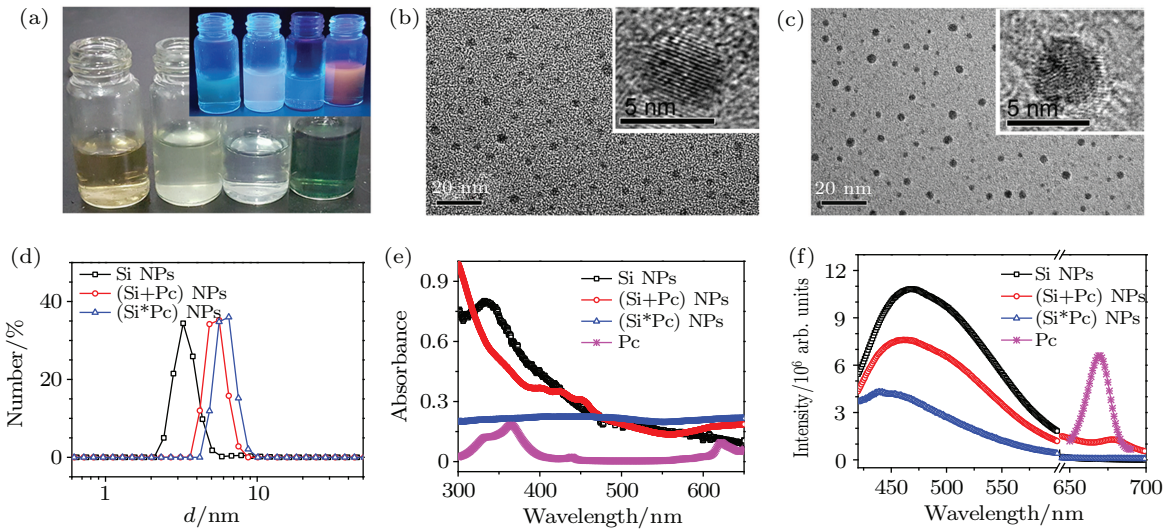


Fig. 1. (color online) Characterizations of pure Si, (Si+Pc), and (Si∗Pc) NPs. (a) Digital images of Si, (Si+Pc), (Si∗Pc) NP dispersions and free Pc (in DMSO) in ambient light or under UV irradiation. (b) and (c) TEM and HR-TEM images of Si and (Si+Pc) NPs. (d)–(f) DLS, UV–vis absorption and fluorescence profiles of Si, (Si+Pc), and (Si∗Pc) NP dispersions. The excitation wavelength in panel (f) is 365 nm.

sizes of 5.6 ± 0.3 nm and 6.5 ± 0.4 nm,than the initial Si NPs (3.8 ± 0.2 nm). UV–vis absorption spectra show the characteristic peaks of Si NPs and free Pc at 334 nm and 622 nm, respectively. Both of these absorption peaks are included in the profile of the (Si+Pc) NPs (Fig. 1(e)). For the (Si∗Pc) NPs, a wide range of absorption is observed. The fluorescence spectra of the (Si+Pc) NPs demonstrate peaks at approximate 460 nm and 679 nm, which are in accordance with the characteristic peaks of Si NPs (at 468 nm) and free Pc (at 669 nm), respectively, although they are somewhat shifted. A similar phenomenon is observed for the (Si∗Pc) NPs with emitting peaks at 445 nm and 680 nm (Fig. 1(f)). These results confirm the successful decoration of Pc to the Si QDs. We attribute the shift in wavelength to the surficial decoration and/or size effects of these nanoparticles.

3.2. Cellular internalization and intracellular localization of Pc-loaded Si NPs

The Si, (Si+Pc) and (Si∗Pc) NPs are co-incubated with MGC-803 cells respectively, for different time durations prior to observation under confocal microscope. The time-dependent transmembrane entry of the nanocomposite NPs was observed (Fig. A1 in Appendix A). Figure 2 shows the confocal images, in the Si, Pc, transmission and merged channels, of representative cells after NP treatment for 24 h (at 1.2 mg·mL^{-1} in respect to Si content). For all the Si, (Si+Pc), and (Si∗Pc) NP systems, the fluorescence of Si is observed in the interior of the cells, probably remaining in the cytoplasm without entering into the nucleus. The fluorescent signals of Pc from the (Si+Pc) and (Si∗Pc) NPs are co-localized well with that of Si, indicating the stable loading of Pc on Si NPs even after cellular internalization. The cells, with internalized NPs, are further treated with LysoTracker Green DND-26 into visualized lysosomes. As shown in Fig. 3(a), the co-localization of fluorescence signals from Si NPs (with loaded Pc) and LysoTracker indicates that the internalized NPs are in the lysosomes at the moment.[1,19] Moreover, the fluorescence signals from both the Si and Pc content promise dual-channel fluorescence imaging of the cells for possible applications in fluorescence imaging-guided cancer therapy.

The fluorescence stability of the internalized NPs is further confirmed by continuous laser exposure *in situ*. The fluorescence intensities in the Si, Pc and commercial LysoTracker channels are analyzed respectively after irradiation of different time durations, both qualitatively and quantitatively (Figs. 3(b) and 3(c)). It is found that the fluorescence of Pc or the LysoTracker begin to dim and quench after around 20 min. However, even after a long irradiation time of 40 min, the fluorescence in the Si channel remains stable. These results indicate the potential applications of the Si NP drug carriers for long-time bioimaging.

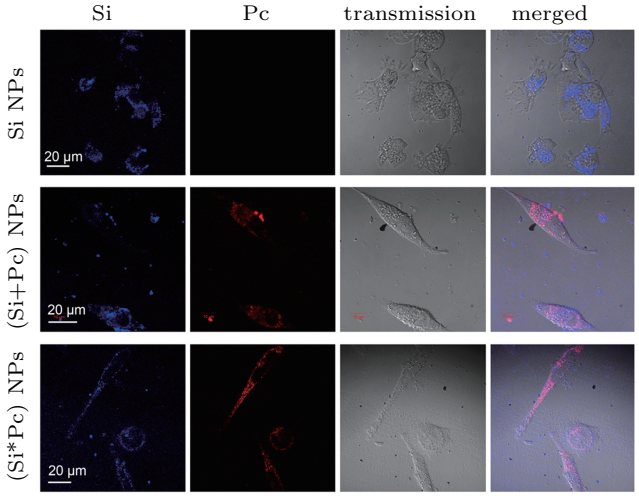


Fig. 2. (color online) Confocal images, including Si, Pc, transmission and merged channels, of the intracellular distribution of Si, (Si+Pc), and (Si∗Pc) NPs in MGC-803 cells after being co-incubated for 24 h at 1.2 mg·mL^{-1} (in respect to Si content).

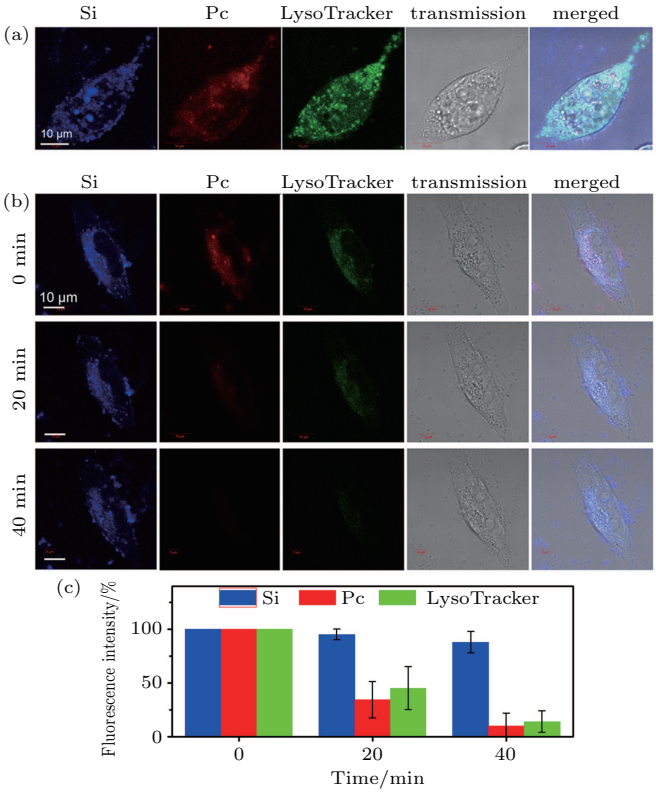


Fig. 3. (color online) Intracellular localization and photostability of (Si+Pc) NPs. (a) Representative MGC-803 cells which are treated with (Si+Pc) NPs for 24 h and labelled with LysoTracker (green fluorescence) for 30 min prior to confocal imaging. (b) Fluorescence stabilities of the Si, Pc, and LysoTracker in cells, under continuous laser exposure for 20 min and 40 min *in situ*. The cells are treated with (Si+Pc) NPs (at 1.2 mg·mL^{-1} for 24 h) and LysoTracker (for 30 min). (c) Time-dependent normalized fluorescence intensity in each channel integrated from panel (b). Error bars are based on the SD of more than 30 cells in three parallel samples.

The cells with internalized NPs show regular morphology which indicates little cytotoxicy of the particles. Quantitative cellular viability analysis after NP treatment for 24 h or 48 h at various NP concentrations from 0 to 260 μg·mL^{-1} in respect to Si content (or from 0 to 40 μg·mL^{-1} for free Pc), based on

the standard MTT test, is shown in Fig. 4. Under all the conditions, a cell viability of above 80% is obtained, which shows a favorable biocompatibility of all the three types of NPs.

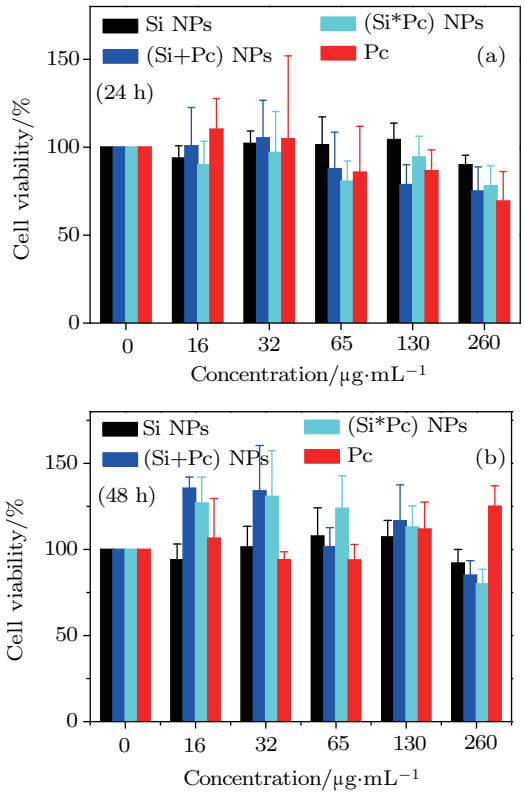


Fig. 4. (color online) Cell viability of MGC-803 cells treated with Si, (Si+Pc), and (Si∗Pc) NPs at various concentrations (from 0 to 260 μg·mL^{-1} in respect to Si content) for (a) 24 h and (b) 48 h. Free Pc is also tested as a control (from 0 to 40 μg·mL^{-1}). Error bar represents the standard deviation of the mean over three duplicate assay features.

3.3. *In vitro* PDT effect test

The Pc is a representative type of PDT drug which can generate reactive oxygen species (ROS) under laser irradiation at a certain wavelength to kill tumor cells. Here, the MGC-803 cells with internalized Si, (Si+Pc), and (Si∗Pc) NPs, are irradiated by a laser (at 610 nm with a power of 25 mW·cm^{-2}) for 30 min and the resulting cells are observed under confocal microscope or analyzed with standard MTT test. The representative images of the cells are shown in Fig. 5. It can be seen that for the pure Si NP group, cells maintain their regular morphology. However, for the (Si+Pc) and (Si∗Pc) NP groups, prominent changes in cellular morphology, such as the vacuolization of the cytoplasm and the blistering of the cell membrane, occur. MTT test shows that ∼ 92% cells treated with (Si+Pc) NPs are destroyed after laser irradiation. Similar results are obtained for the (Si∗Pc) NP group (at ∼ 85%). Note that even after laser treatment the fluorescence of Pc keeps co-localizing well with Si. These results demonstrate that the Pc loaded on Si NPs, both through physical adsorption or chemical binding, has good PDT effect against tumor cells even without being released from the drug carriers.

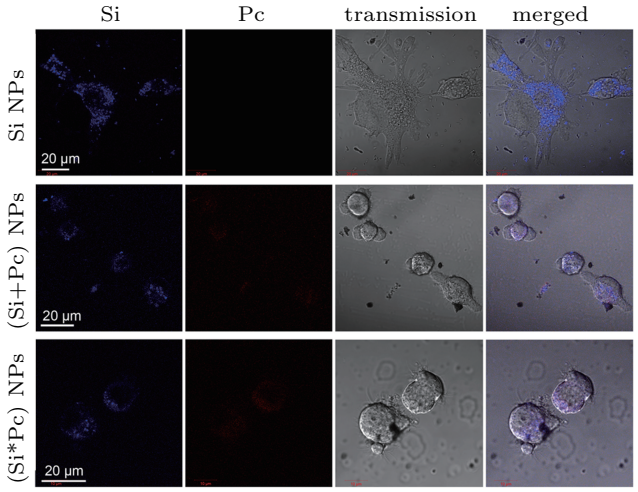


Fig. 5. (color online) *In vitro* PDT effects of MGC-803 cells with Si, (Si+Pc), and (Si∗Pc) NPs. The cells are treated with NPs (at 1.2 mg·mL^{-1} in respect to Si) for 24 h and exposed to a laser (at 610 nm) for 30 min.

3.4. *In vivo* anti-tumor experiments

Mice bearing MGC-803 tumor at their back are used as models to testify the *in vivo* anti-tumor effect of the Si NP-based nanocomposite drugs. Representative images of the mouse are shown in Fig. 6(a) and the time-dependent changes

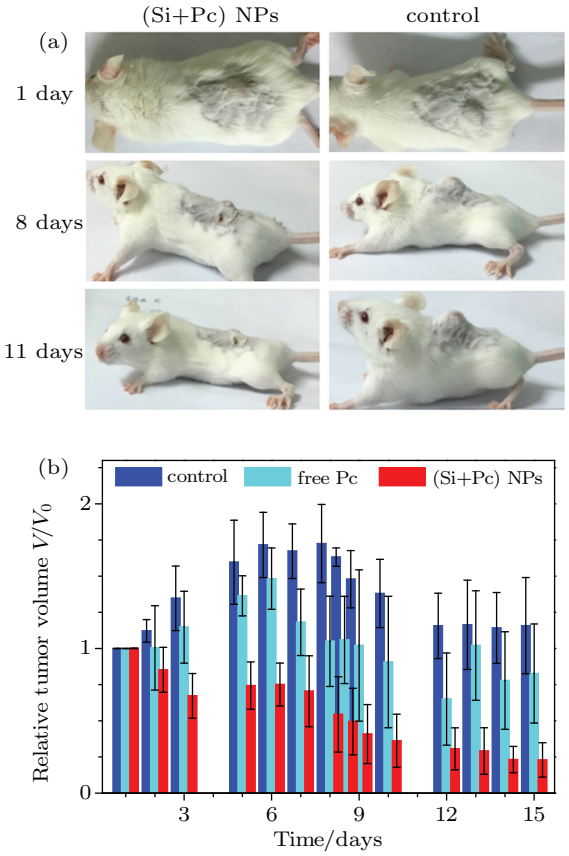


Fig. 6. (color online) Inhibition of tumor growth by (Si+Pc) NPs. (a) Representative photos of MGC-803 tumor bearing mice on different days during PDT treatment. (b) Quantitatively time-dependent distribution of tumor size. The solutions, including PBS, (Si+Pc) NP dispersion and free Pc, are injected on the 1st day and 7th day followed by 30 min NIR exposure each time after injection. Error bars are based on the SD of triplicated samples.

in the normalized tumor size based on triplicated samples are plotted in Fig. 6(b). In comparison with the PBS group, the tumor after free Pc treatment decreases in size to around 80% after 15 days. However, for the (Si+Pc) NP group, the size of the tumor decreases obviously and is almost distinguishable after a shorter treatment of 15 days. These results demonstrate the efficient delivery of the water-insoluble Pc on Si NPs for photo dynamic therapy against tumor.

4. Conclusions and perspectives

In this work, we produce a type of water-dispersible Si QD, and the hydrophobic drug Pc is efficiently loaded on the Si QDs via facile preparation such as physical adsorption or chemical conjugation. The as-obtained Si/Pc nanocomposite particles are well water-dispersible and have small sizes below 5 nm. They can be effectively uptaken by cells while show feasible cytotoxicity, and maintain stable even after cell internalization. The composite particles are imaged by dual-channel fluorescence signals in Si and Pc channels. We find that the fluorescence in the Si channel shows robust stability promising its applications for long-time tracking and bioimaging. More interestingly, the composite nanoparticles demonstrate significant PDT anti-tumor effects both *in vitro* and *in vivo*. Based on the Si QDs, these results provide a novel strategy for the efficient delivery of hydrophobic drugs and their use for fluorescence imaging guided photo dynamic therapy against tumors.

Appendix A: supporting information

Figure A1 gives the time-dependent transmembrane entry of the nanocomposite NPs.

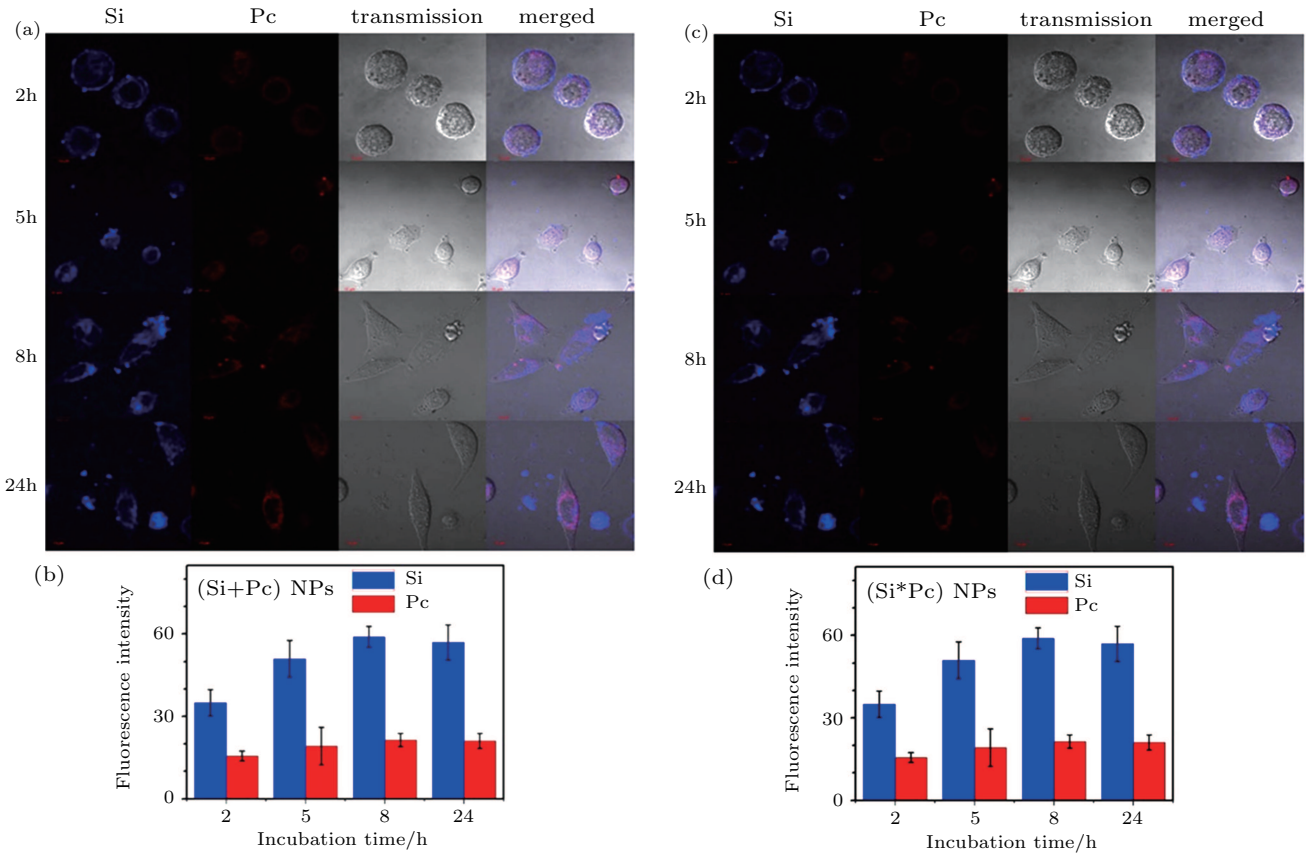


Fig. A1. (color online) Confocal images of MGC-803 cells co-incubated with (a) (Si+Pc) or (c) (Si∗Pc) NPs for 2 h, 5 h, 8 h, and 24 h. (b) and (d) The corresponding distribution of mean fluorescence intensity within one cell, in Si or Pc channel, is quantitatively analyzed. Error bars are based on the SD of more than 30 cells in three parallel samples. The increase in fluorescence intensity corresponds to an increase in the number of fluorescence particles internalized within cells.

Acknowledgment

The authors sincerely thank Prof. Yao He and Bin Song (Institute of Functional Nano and Soft Materials (FUNSOM), Soochow University) for their kind help in the Si QD synthesis and TEM characterizations and also the *in vivo* experiments.

References

[1] Ji X, Peng F, Zhong Y, Su Y, Jiang X, Song C, Yang L, Chu B, Lee S T and He Y 2015 *Adv. Mater.* **27** 1029

[2] Jiang S, Gnanasammandhan M K and Zhang Y 2010 *J. R. Soc. Interface* **7** 3

[3] Su H Y, Wu C Q, Li D Y and Ai H 2015 *Chin. Phys. B* **24** 127506

[4] Gao M, Yu F, Lv C, Choo J and Chen L 2017 *Chem. Soc. Rev.* **46** 2237

[5] Yukawa H and Baba Y 2017 *Anal. Chem.* **89** 2671

[6] Haque A, Faizi M S, Rather J A and Khan M S 2017 *Bioorg. Med. Chem.* **25** 2017

[7] Luo Z, Cai K Y, Hu Y, Zhao L, Liu P, Duan L and Yang W H 2011 *Angew. Chem. Int. Ed. Engl.* **50** 640

[8] Pan L M, He Q J, Liu J N, Chen Y, Ma M, Zhang L L and Shi J L 2012 *J. Am. Chem. Soc.* **134** 5722

[9] Wang W W, Cheng D, Gong F M, Miao X M and Shuai X T 2012 *Adv. Mater.* **24** 115

[10] Senapati L, Schrier J and Whaley K B 2004 *Nano Lett.* **4** 2073

[11] Su Y Y, Peng F, Jiang Z Y, Zhong Y L, Lu Y M, Jiang X X, Huang Q, Fan C H, Lee S T and He Y 2011 *Biomaterials* **32** 5855

[12] Zhong Y L, Peng F, Bao F, Wang S Y, Ji X Y, Yang L, Su Y Y, Lee S T and He Y 2013 *J. Am. Chem. Soc.* **135** 8350

[13] Zhong Y, Peng F, Wei X, Zhou Y, Wang J, Jiang X, Su Y, Su S, Lee S T and He Y 2012 *Angew. Chem. Int. Ed. Engl.* **51** 8485

[14] Park J H, Gu L, Von Maltzahn G, Ruoslahti E, Bhatia S N and Sailor M J 2009 *Nat. Mater.* **8** 331

[15] Wang Z, Zhang G F, Li B, Chen R Y, Qin C B, Xiao L T and Jia S T 2015 *Acta Phys. Sin.* **64** 247803 (in Chinese)

[16] Abbasi S, Servatkhah M and Keshtkar M M 2016 *Chin. Phys. B* **25** 087301

[17] An D Y, Su J G, Li C H and Li J Y 2015 *Chin. Phys. B* **24** 120504

[18] Liu J, Wang R, Wu S, Yuan B, Bao M, Li J, Dou Y, He Y and Yang K 2017 *Nanotechnology* **28** 135601

[19] Peng F, Su Y Y, Ji X Y, Zhong Y L, Wei X P and He Y 2014 *Biomaterials* **35** 5188.

[20] Peng F, Su Y Y, Zhong Y L, Fan C H, Lee S T and He Y 2014 *Acc. Chem. Res.* **47** 612

[21] Tallury P, Payton K and Santra S 2008 *Nanomedicine* **3** 579

[22] Li Y, Wang X B, Fan Z Q and Li X J 2014 *Chin. Phys. Lett.* **31** 047801

[23] Kinnari P J, Hyvönen M L K, Mäkilä E M, Kaasalainen M H, Rivinoja A, Salonen J J, Hirvonen J T, Laakkonen P M and Santos H A 2013 *Biomaterials* **34** 9134

[24] Hochbaum A I, Gargas D, Hwang Y J and Yang P 2009 *Nano Lett.* **9** 3550

[25] Shao M, Cheng L, Zhang X, Ma D D and Lee S T 2009 *J. Am. Chem. Soc.* **131** 17738

[26] Cheng Y, C Samia A, Meyers J D, Panagopoulos I, Fei B and Burda C 2008 *J. Am. Chem. Soc.* **130** 10643

[27] Ince M, Er O, Ocakoglu K, Lambrecht F Y, Colak S G, Soylu H M, Kayabasi C and Gunduz C 2016 *Chem. Biol. Drug Des.* **87** 224

[28] Yu C, Meyers J D, Broome A M, Kenney M E, Basilion J P and Burda C 2011 *J. Am. Chem. Soc.* **133** 2583

[29] Zorlu Y, Dumoulin F, Bouchu D, Ahsen V and Lafont D 2010 *Tetrahedron Lett.* **51** 6615

[30] Li J, Zhang W D, Hu Z J, Jiang X J, Ngai T, Lo P C, Zhang W and Chen G J 2013 *Polym. Chem.* **4** 782

[31] Cheng L, He W W, Gong H, Wang C, Chen Q, Cheng Z P and Liu Z 2013 *Adv. Funct. Mater.* **23** 5893